nature neuroscience

ARTICLES

https://doi.org/10.1038/s41593-017-0005-0

Activation of planarian TRPA1 by reactive oxygen species reveals a conserved mechanism for animal nociception

Oscar M. Arenas[1], Emanuela E. Zaharieva[1], Alessia Para[1], Constanza Vásquez-Doorman[2], Christian P. Petersen[2] & Marco Gallio[1*]

All animals must detect noxious stimuli to initiate protective behavior, but the evolutionary origin of nociceptive systems is not well understood. Here we show that noxious heat and irritant chemicals elicit robust escape behaviors in the planarian *Schmidtea mediterranea* and that the conserved ion channel TRPA1 is required for these responses. TRPA1-mutant *Drosophila* flies are also defective in noxious-heat responses. We find that either planarian or human TRPA1 can restore noxious-heat avoidance to TRPA1-mutant *Drosophila*, although neither is directly activated by heat. Instead, our data suggest that TRPA1 activation is mediated by H_2O_2 and reactive oxygen species, early markers of tissue damage rapidly produced as a result of heat exposure. Together, our data reveal a core function for TRPA1 in noxious heat transduction, demonstrate its conservation from planarians to humans, and imply that animal nociceptive systems may share a common ancestry, tracing back to a progenitor that lived more than 500 million years ago.

Each animal group uses specialized sensory systems to detect and avoid predators and to find food sources and mates. Due to specific demands, sensory systems evolve independently in different species. Yet while each animal group lives in a sensory world that is essentially unique, most of what we know about sensory representation comes from a very limited number of species—a handful of vertebrate and invertebrate model systems.

The detection of potentially harmful conditions is a core sensory task. The ion channel TRPA1 is remarkably conserved across animal evolution and has been implicated in responses to a broad range of electrophilic irritant chemicals, as well as to noxious hot or cold temperatures in humans[1], mice[2–8], and flies[2,9,10]. Notably, while TRPA1's sensitivity to irritant chemicals has been widely conserved[11] (in all but the *C. elegans* homolog[12]), its temperature gating appears to have changed repeatedly during evolution[13]. In vitro, some mammalian TRPA1 homologs are activated by noxious cold[14], while others are insensitive to temperature (reviewed in ref. [13]). In contrast, TRPA1 from chicken[15], various reptiles, and *Xenopus* frogs are activated by warm temperatures[16,17], and the zebrafish genome encodes two distinct paralogs, only one of which shows thermosensory responses[18,19]. The situation in invertebrates is also complex: while *C. elegans* TRPA1 is activated by cold[12], insect TRPA1s (honeybee[20], mosquito[21], etc.) are activated by warm temperatures, and the fruit fly homolog is spliced into at least four variants[10], including heat-sensitive and heat-insensitive ones[2,10,22].

What is the ancestral function of TRPA1? How ancient is its association with nociceptors? Planarian flatworms are an attractive system in which to study evolutionary origins of sensory transduction. As members of the phylum Platyhelminthes, planarians are considered among the simplest animals with bilateral symmetry and a centralized nervous system. From an evolutionary perspective, they are very distant from taxa that include extensively studied species such as nematodes, flies, and mice (ref. [23] and Fig. 1a). Furthermore, recent work on regeneration has led to the development of RNA interference (RNAi) protocols to systemically knock down the expression of selected genes in vivo[24]. Here we use these tools to investigate the function of TRPA1 in the freshwater planarian *S. mediterranea*.

Results

S. mediterranea TRPA1 mediates noxious heat avoidance

A fragment of the *S. mediterranea TRPA1* gene has been previously used in in-situ hybridization experiments as a marker for a subset of differentiated neurons[25]. Starting from this fragment, we cloned a full-length coding sequence for the gene (see Methods for details), henceforth referred to as *Smed-TRPA1* (Fig. 1b). To test whether *Smed-TRPA1* mediated the avoidance of noxious heat in *S. mediterranea*, we designed a two-choice avoidance assay (Supplementary Fig. 1) based on one we previously developed for fruit flies[26]. Animals were introduced into a small circular chamber covered by a thin film of water and were tracked while making a choice between floor tiles kept at moderate (24 °C) or hot (32 °C) temperatures; the time spent in each quadrant was then quantified to calculate an avoidance index. In this assay, *S. mediterranea* showed robust avoidance of heat (32 °C, avoidance index ≈ 1), manifested as sharp turns away from the hot quadrants (Fig. 1c). This is consistent with a nocifensive behavior and indeed with the fact that *S. mediterranea* comes from cool-water environments and can die from brief exposure to 35 °C[27] (data not shown).

Notably, the avoidance of hot quadrants was severely disrupted by RNAi knockdown of *Smed-TRPA1* (Fig. 1c,d and Supplementary Video 1). *Smed-TRPA1* RNAi animals glided around the chamber without turning at the hot–cold boundaries (Fig. 1c) and, overall, spent nearly as much time in hot quadrants as in cool quadrants. This stood in sharp contrast with the behavior of both untreated worms and control worms (i.e., worms fed double-stranded RNA

[1]Department of Neurobiology, Northwestern University, Evanston, IL, USA. [2]Department of Molecular Biosciences, Northwestern University, Evanston, IL, USA. *e-mail: marco.gallio@northwestern.edu

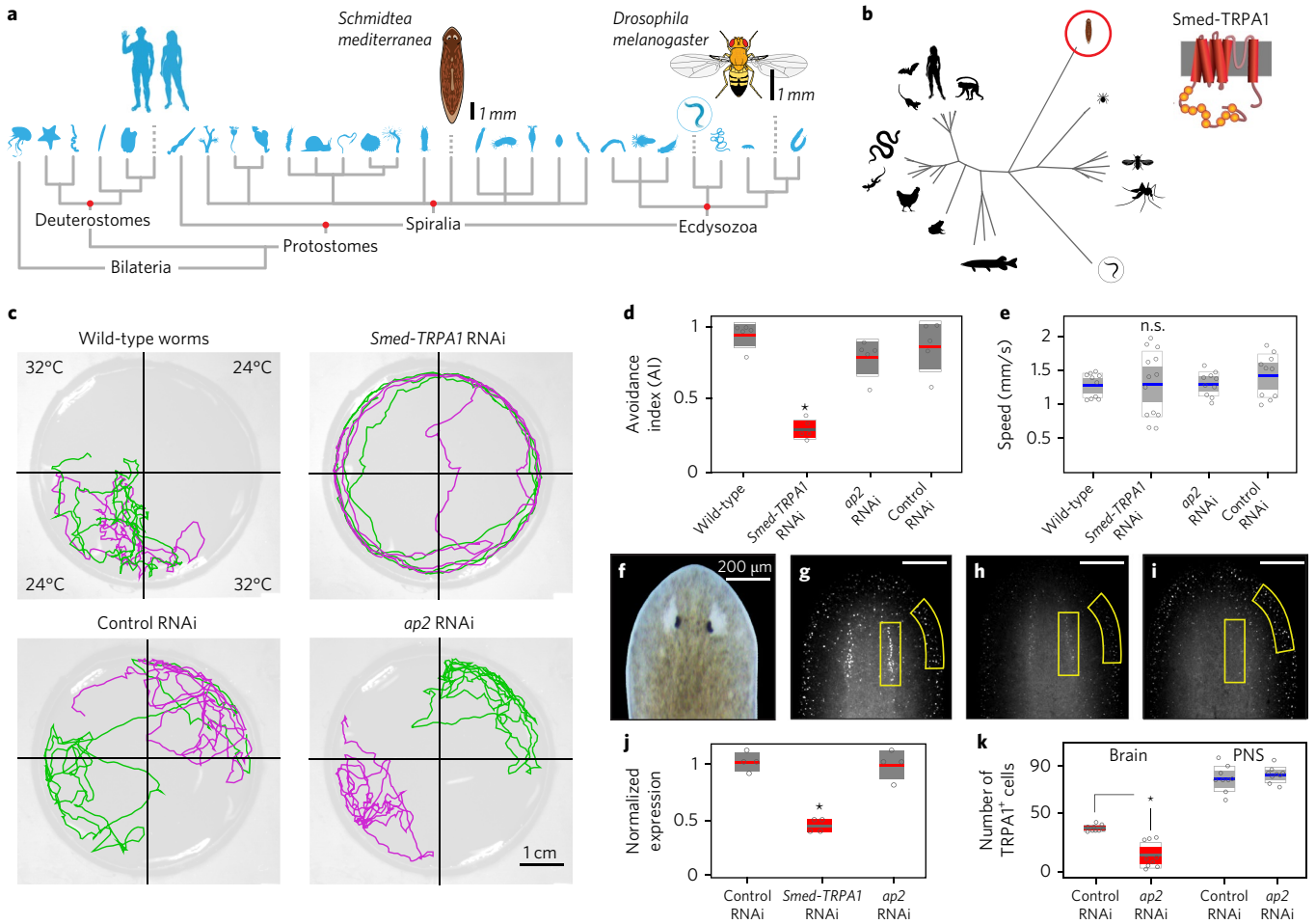

Fig. 1 | *Smed-TRPA1* is required for noxious heat avoidance in the planarian worm *S. mediterranea*. **a**, Phylogeny of Bilateria, showing the position of *Schmidtea* (*C. elegans* is circled). **b**, Phylogenetic tree constructed from an alignment of full-length TRPA1 protein sequences from a variety of species. The source of Smed-TRPA1 is circled and a model of the channel's structure is shown (circles, ankyrin repeats; cylinders, transmembrane domains). **c**, Two-choice assay for heat avoidance. In each trial, two opposing floor tiles are set to 24 °C and two to 32 °C (noxious heat). Tracks of two worms during one such trial are shown in green and purple. Unlike wild-type worms, controls (*unc22* RNAi), and *ap2* RNAi worms, *Smed-TRPA1* RNAi animals were not confined to the cool quadrants. **d**, Avoidance index for 32 °C for RNAi animals. *Smed-TRPA1* RNAi animals show a reduced avoidance index for heat ($n = 5$ groups of 10 animals each, $^*P = 0.0054$, Kruskal-Wallis; $\chi^2_{3,16} = 12.68$). **e**, *Smed-TRPA1* RNAi does not impact the animal's speed of movement ($n = 10$–13 animals; n.s., not significantly different, $P = 0.6$, Kruskal-Wallis; $\chi^2_{3,39} = 1.48$). **f**–**i**, In situ hybridization (head region; overview shown in (**f**)) with a *Smed-TRPA1* probe in (**g**) control (*unc22*) RNAi, (**h**) *Smed-TRPA1* RNAi, and (**i**) *ap2* RNAi animals demonstrates overall reduction of mRNA by *Smed-TRPA1* RNAi (independent quantification by quantitative PCR (q-PCR) is shown in (**j**); $n = 4$ replicates of 3 animals each, $^*P = 0.02$, Kruskal-Wallis; $\chi^2_{2,9} = 7.65$). **k**, In contrast, *ap2* RNAi reduces the number of *Smed-TRPA1*-expressing cells in the brain region but not in the periphery ($n = 9$ animals, $^*P = 1.5 \times 10^{-5}$; unpaired *t* test, $t_{16} = 6.1048$); in all plots: line, mean; outer boxes, ±1 s.d.; inner boxes, 95% confidence interval. PNS, peripheral nervous system.

(dsRNA) targeted to a sequence not present in the worm genome; Fig. 1c,d). Notably, *Smed-TRPA1* RNAi worms glided around the chamber at speeds comparable to those of controls (Fig. 1e) and displayed robust negative phototaxis when given a choice between light and dark (in an independent assay; Supplementary Fig. 2), indicating that *Smed-TRPA1* RNAi did not mar gross locomotor functions, nor did it impact all aversive behavior.

RNAi knockdown of the transcription factor AP2 has been previously shown to impair the expression of TRPA1 in *S. mediterranea*[25]. Based on this, we reasoned that *ap2* RNAi could provide an independent means to assess the role of TRPA1 in heat nociception. Unexpectedly, *ap2* RNAi animals did not display an avoidance defect and instead avoided the hot quadrants as robustly as controls (Fig. 1c,d). In situ hybridization revealed that *ap2* RNAi was effective in knocking down *Smed-TRPA1* expression only within the brain and not in peripheral neurons (Fig. 1f–k). The fact that animals with significantly reduced *Smed-TRPA1* expression within the brain behaved normally suggests that *Smed-TRPA1* is required at the periphery for the detection or responses to noxious heat.

Smed-TRPA1 is also required for chemical nociception

Next, we tested *Smed-TRPA1*-knockdown animals for potential defects in chemical nociception by assaying behavioral responses to allyl isothiocyanate (AITC). AITC is the agent responsible for the pungent taste of mustard and wasabi, and it is a well-known chemical agonist of TRPA1[3,4,8]. We developed an arena consisting of circular chambers interconnected by small corridors that are not readily traversed by the worms (Fig. 2a). Animals fed control dsRNA (see above) or *Smed-TRPA1* dsRNA were introduced in the first chamber in the presence of a mock agar pellet or, alternatively, an agar pellet laced with AITC; their behavior was then monitored for 5 min. Mock pellets were readily explored by untreated animals as well as by RNAi controls, which, as a result, remained in their vicinity. In contrast, AITC produced strong aversive responses, including rapid

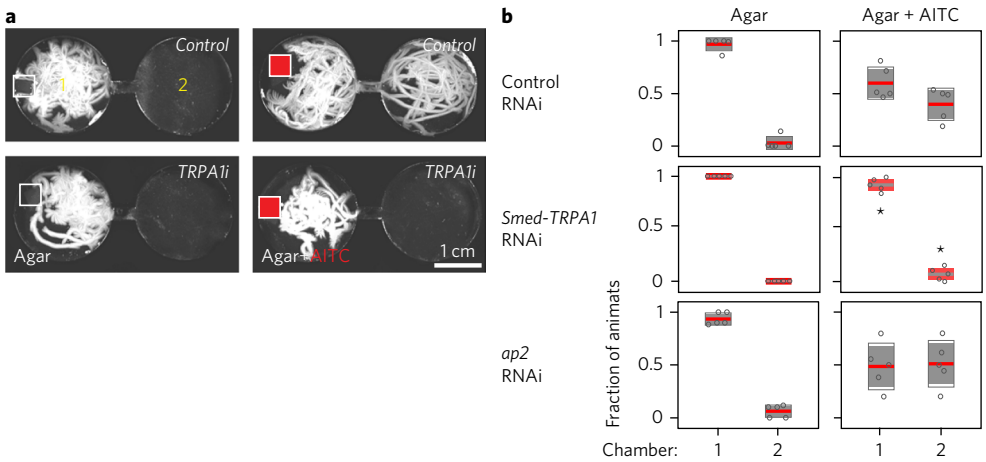

Fig. 2 | *Smed-TRPA1* is required for behavioral avoidance of the irritant chemical AITC. a, The two-chamber arena designed to quantify behavioral avoidance of chemical agonists of TRPA1. Planarian worms were introduced in chamber 1 in the presence of a mock agar pellet (empty squares) or an agar + AITC pellet (50 mM; red squares); their movement was then recorded for 5 min. The panels show maximum projections of 5-min movies, illustrating the extent of worm movement (white tracks). TRPA1i, *Smed-TRPA1* RNAi worms. **b**, In the presence of agar alone, control (*unc22*), *ap2* RNAi, and *Smed-TRPA1* RNAi worms do not readily cross the narrow channel connecting chambers 1 and 2. In the presence of AITC, both control (*unc22*) and *ap2* RNAi worms exit chamber 1 and explore chamber 2. In contrast, *Smed-TRPA1* RNAi animals overwhelmingly remain in chamber 1 ($n = 5$ groups of 10 animals each; fraction was calculated on the last 1 min of video; $^*P = 0.0078$, Kruskal-Wallis comparing fraction of animals in chamber 1 or 2 across treatments; $\chi^2_{2,12} = 9.71$; line, mean; outer boxes, ±1 s.d.; inner boxes, 95% confidence interval).

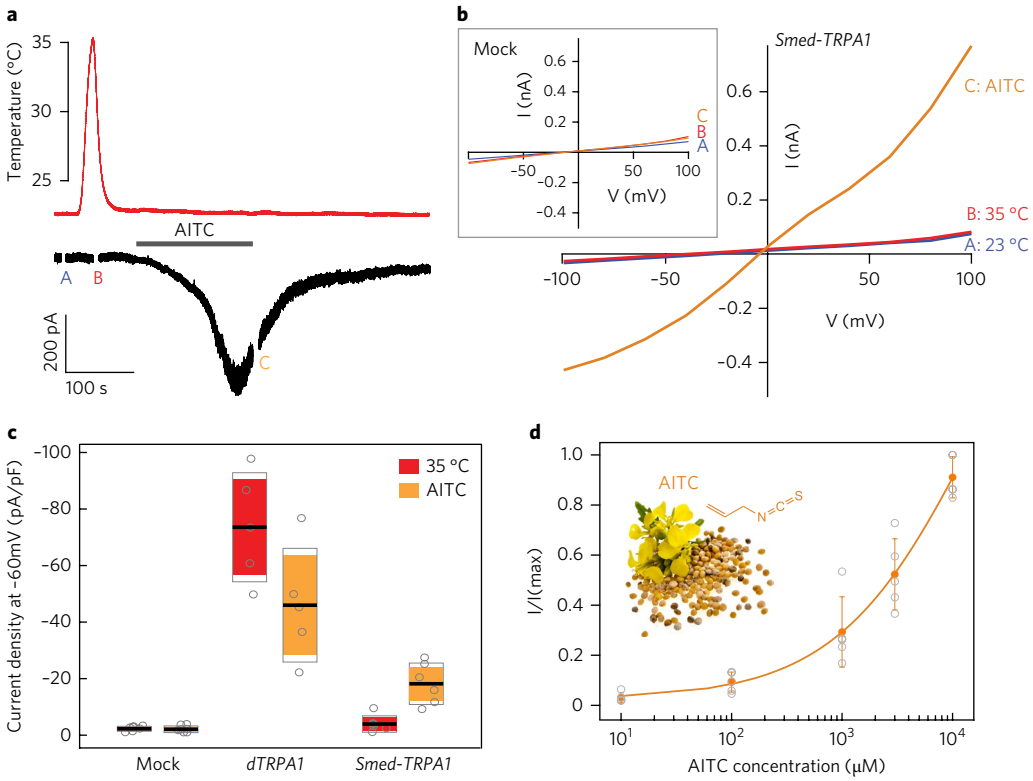

Fig. 3 | *Smed-TRPA1* expressed in *Drosophila* cells is activated by AITC but not by heat. a, S2R+ *Drosophila* cells voltage-clamped at −60 mV were stimulated by heat (red trace) and by bath application of AITC (500 μM, gray bar). AITC application (but not heating) resulted in an inward current. **b**, Current–voltage relationship from averages of $n = 3$ consecutive voltage-step protocols done at room temperature (23 °C; blue trace), during the heat stimulation (red trace), and at the end of AITC application (orange trace; note that the inset is from a mock transfected cell; the timing of each set of measurements is also labeled A, B and C on the trace shown in **a**). **c**, Current density (max ÷ capacitance) at 32 °C and in the presence of AITC recorded in mock-transfected, *dTRPA1-A* transfected, and *Smed-TRPA1* transfected cells (line, mean; outer boxes, ±1 s.d.; inner boxes, 95% confidence intervals). **d**, Dose-response graph for AITC activation of Smed-TRPA1 (yellow dots and bars, average ± s.d.; $n = 5$ cells per condition; mustard flower and seeds represent an iconic source of AITC).

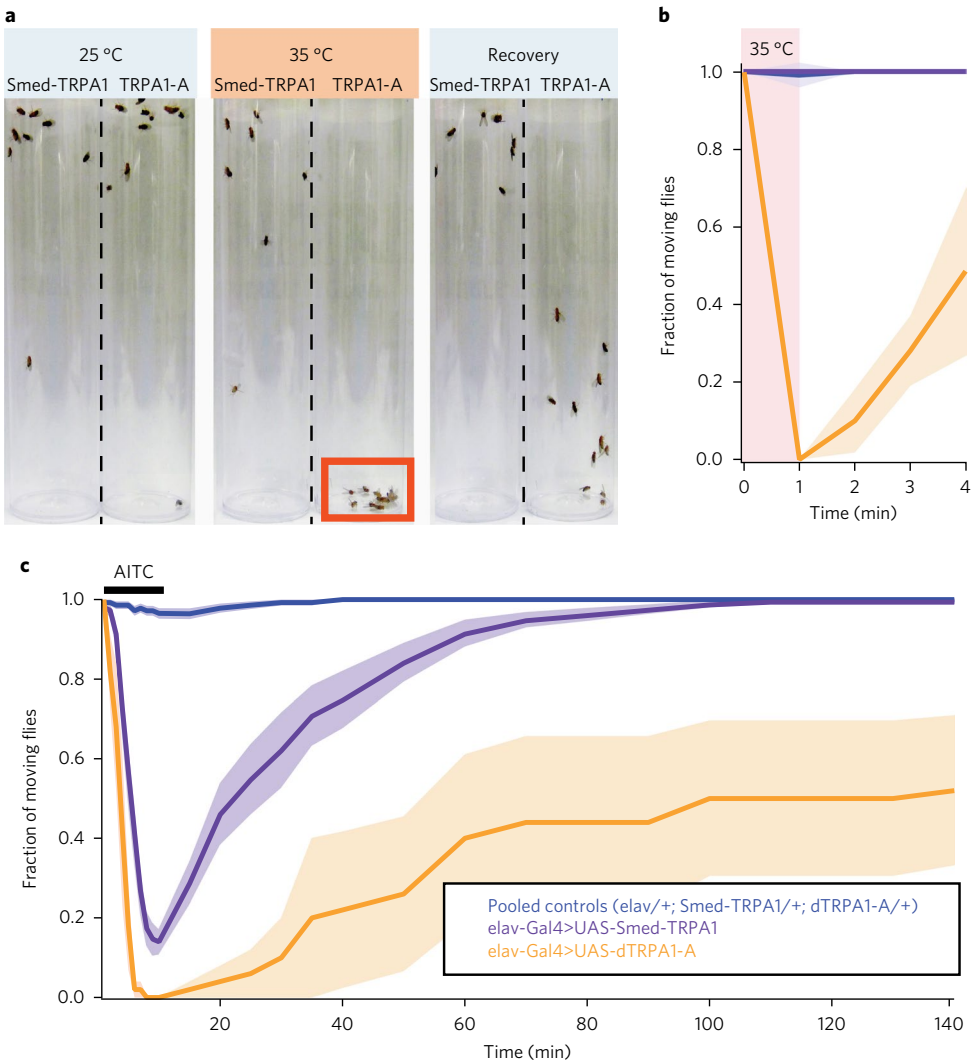

Fig. 4 | Functional expression of Smed-TRPA1 in vivo in adult *Drosophila* further demonstrates that the channel is sensitive to AITC but not to heat (°C). **a**, Adult fruit flies expressing either Smed-TRPA1 or, as a control, the intrinsically heat-sensitive *Drosophila* TRPA1-A splice variant throughout the nervous system (under the control of elav-Gal4) were subjected to a brief step at 35 °C (a temperature that does not normally impair fly activity). TRPA1-A-expressing flies are readily and reversibly incapacitated by heat (presumably because of simultaneous depolarization of neurons, caused by channel opening) and fall to the bottom of the tube (orange box); Smed-TRPA1 flies appear instead unaffected. **b**, Quantification of the experiment in **a**. Blue trace, pooled controls (elav/+, UAS-Smed-TRPA1/+, and UAS-TRPA1-A/+; $n = 4$ groups of 10 animals each, tested separately); purple trace, experimental animals (elav-Gal4>UAS-Smed-TRPA1; $n = 4$ groups of 10 animals each); orange trace, positive control (elav-Gal4>UAS-TRPA1-A; $n = 4$ groups of 10 animals each; for all traces, shaded area shows ± s.e.m.; note that blue and purple traces overlap). **c**, Adult flies expressing either Smed-TRPA1 or TRPA1-A were reversibly incapacitated by brief exposure to AITC vapors (Methods; groups and n values as above; shaded area shows ± s.e.m.).

withdrawal and abrupt turns. The worms ultimately escaped away from the chamber containing the pellet by traversing the narrow corridors (Fig. 2b and Supplementary Video 2). Again in sharp contrast to controls, *Smed-TRPA1*-knockdown animals did not display aversive responses and instead remained in the first chamber, in the vicinity of the AITC-laced pellet (Fig. 2b).

Heterologously expressed Smed-TRPA1 responds to AITC but not heat

Our experiments show that *Smed-TRPA1* is a key mediator of both heat avoidance and chemical nociception in vivo in *S. mediterranea*. To begin studying the biophysical properties of the channel in vitro, we next performed whole-cell patch-clamp electrophysiology on cells heterologously expressing *Smed-TRPA1*. To achieve functional expression of Smed-TRPA1, we chose *Drosophila* S2 cells, a system previously used for *Drosophila* TRPA1[28]. Our recordings show that, in S2 cells, Smed-TRPA1 was activated by AITC (Fig. 3). In contrast, the channel was not directly gated by heat (Fig. 3a–d). Even when misexpressed in vivo, in transgenic *Drosophila* (i.e., in all fly neurons), Smed-TRPA1 could be readily activated by AITC but not by heat (Fig. 4). As a control, the *Drosophila* TRPA1-A variant[10] was activated by both AITC and heat in both contexts (Figs. 3c,d and 4, and ref. [29]).

Across-phylum rescue of *Drosophila* TRPA1 mutants by distant homologs

The lack of thermal sensitivity of *Smed-TRPA1* in vitro (vis-à-vis the effect of RNAi on noxious heat avoidance) appears puzzling. However, TRPA1 is well known to function both as a primary temperature receptor as well as a signal transduction component, i.e., downstream of diverse signaling events[7,30]. Notably, both the heat-nociception phenotype of *TRPA1*-mutant fly larvae

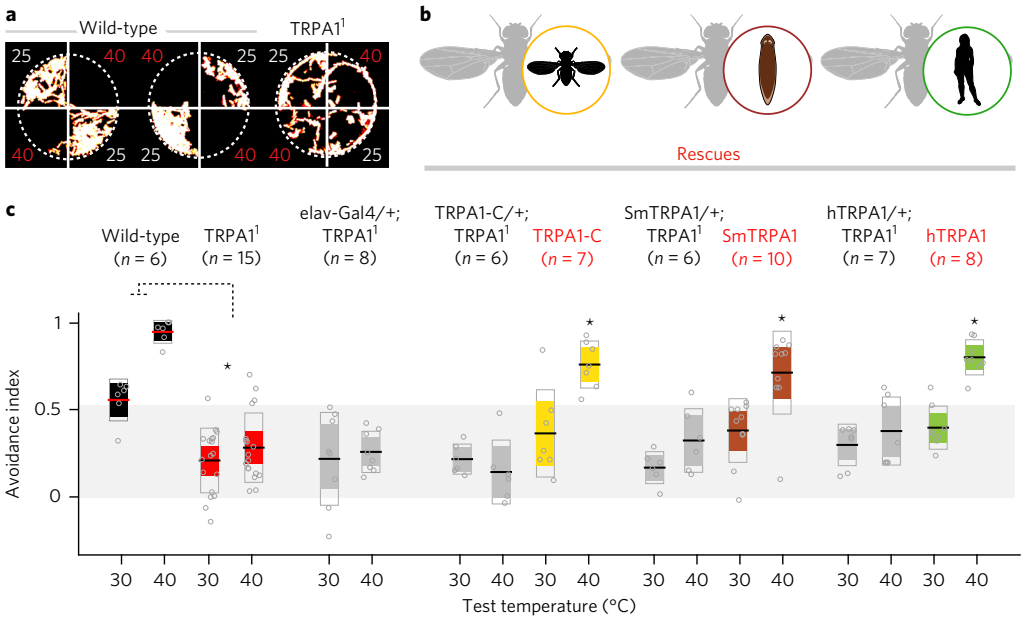

Fig. 5 | Across-phylum rescue of *Drosophila* TRPA1 mutant phenotypes by planarian and human TRPA1. a, In a two-choice assay, wild-type *Drosophila* flies robustly avoid noxious heat (40 °C). In contrast, TRPA1¹ mutants more readily explore the 40 °C quadrants (panels show maximum projections of 3-min movies, illustrating the extent of fly movement; temperature in °C is indicated next to each quadrant). **b**, Schematic of the rescue experiments. **c**, Avoidance index (AI) of wild-type flies (black), TRPA1¹ mutants (red), rescues (yellow, brown, green), and control genotypes (grey). TRPA1¹ mutants displayed a significantly lower avoidance index for heat (unpaired *t* tests, 30 °C: $*P = 4.2 \times 10^{-4}$, $t_{19} = 4.2578$; 40 °C: $*P = 7.7 \times 10^{-7}$, $t_{19} = 7.1991$). Pan-neural expression (under the control of elav-Gal4) of mRNA encoding *Drosophila* TRPA1-C (a splice variant encoding a channel that is not heat-sensitive; yellow), Smed-TRPA1 (brown), or human TRPA1 (green; each under a UAS promoter) significantly rescues noxious heat avoidance (40 °C). Control genotypes: *elav driver/+;TRPA1¹* and *UAS-transgene/+;TRPA1¹* (see Methods for full genotypes). For rescues, AI values for each test temperature were compared by two-way ANOVA; asterisks denote significant interactions between the Gal4 and UAS transgene (from left: $*P = 0.0001$, $F_{1,32} = 19.32$; $*P = 0.0092$, $F_{1,35} = 7.6$; $*P = 0.0011$, $F_{1,34} = 12.7$). Thick line, mean; outer boxes, ±1 s.d.; inner boxes, 95% confidence interval.

and heat-entrainment defects of adults were readily rescued by a non-heat-sensitive variant of the fly TRPA1 (TRPA1-C)[10,31]. These observations led us to directly test the possibility that the non-heat-sensitive Smed-TRPA1 could also substitute for the fly TRPA1, i.e., to attempt across-phylum rescue of a *Drosophila TRPA1*-mutant by expression of the planarian homolog.

First, we used a rapid two-choice assay for temperature preference[26] (similar to that described above) and probed the responses of wild-type and TRPA1-mutant *Drosophila* to both innocuous (30 °C) and noxious (40 °C) heat (Fig. 5a). Consistent with previous reports[9], in our assay *TRPA1*-mutant flies showed a clear defect in the avoidance of noxious heat (Fig. 5a,c; note that residual heat avoidance is likely mediated by *GR28b.d*, a distinct molecular heat receptor[32]). Much like in the larva, this nociceptive phenotype could be significantly rescued by ubiquitous expression of *TRPA1-C*, which encodes a TRPA1 variant not directly activated by heat[10] (Fig. 5b,c). Strikingly, a comparable degree of rescue could be achieved by ubiquitous expression of the planarian *Smed-TRPA1* (34% identical and 53% similar to the fly TRPA1 in amino-acidic sequence; Fig. 5b,c) and even of a human *TRPA1* cDNA (which encodes a protein 36% and 31% identical and 57% and 49% similar to fly and Smed-TRPA1, respectively; Fig. 5b,c).

Hydrogen peroxide and reactive oxygen species as potential mediators of TRPA1 activation

Rescue of the fly phenotype by an evolutionarily distant heat-insensitive homolog such as *Smed-TRPA1* and by human TRPA1 (which is activated by cold rather than heat) argue that the function of TRPA1 in heat nociception is unlikely to be fully explained by direct heat gating. Instead, a number of observations point towards early markers of tissue damage as potential mediators of TRPA1 activation during nociceptive heat responses. Hydrogen peroxide (H_2O_2) is amongst the earliest known markers of mechanical tissue damage in vertebrates[33], *Drosophila*[34], and planarians[35]. H_2O_2, together with additional reactive oxygen species (ROS)[36], is a well-known activator of mammalian and *Drosophila* TRPA1[37–40], and recent work suggest that responses to potentially damaging short-wavelength UV light occur through photochemical production of H_2O_2 and require TRPA1 in both flies[38–41] and planarians[42]. Thus, if noxious heat were to cause rapid, localized production of H_2O_2 and/or ROS, this could provide the direct signal for TRPA1 activation that mediates nociceptive responses.

For this hypothesis to be correct, a number of conditions have to be met: (i) Smed-TRPA1 (like its human and *Drosophila* counterparts) should be activated by H_2O_2; (ii) in vivo, heat stimulation in the appropriate range should cause rapid H_2O_2 and/or ROS production (on a timescale compatible with the animal's escape behaviors); and (iii) if indeed nociceptive heat responses are mediated by H_2O_2 and/or ROS, an acute increase in H_2O_2 and/or ROS levels should sensitize the animal's behavioral responses to noxious heat, and this sensitization should depend on TRPA1. Our experiments confirm each of these predictions.

First, we tested Smed-TRPA1 for potential responses to H_2O_2 in vitro in our cell-expression system (see above). Our recordings showed that, in S2 cells, Smed-TRPA1 was indeed activated by a range of H_2O_2 concentrations (Fig. 6a,b), as was the *Drosophila* counterpart TRPA1-C (i.e., the heat-insensitive fly variant, which also supported behavioral rescue in our experiment; Fig. 6b). We note that, while it is difficult to speculate on the H_2O_2 and ROS concentrations that TRPA1 may encounter during a heat challenge in vivo, secondary modifications (such as prolyl hydroxylation[43]) have been shown to dramatically increase TRPA1 responses to H_2O_2 and/or ROS, potentially expanding the effective sensitivity of the channel.

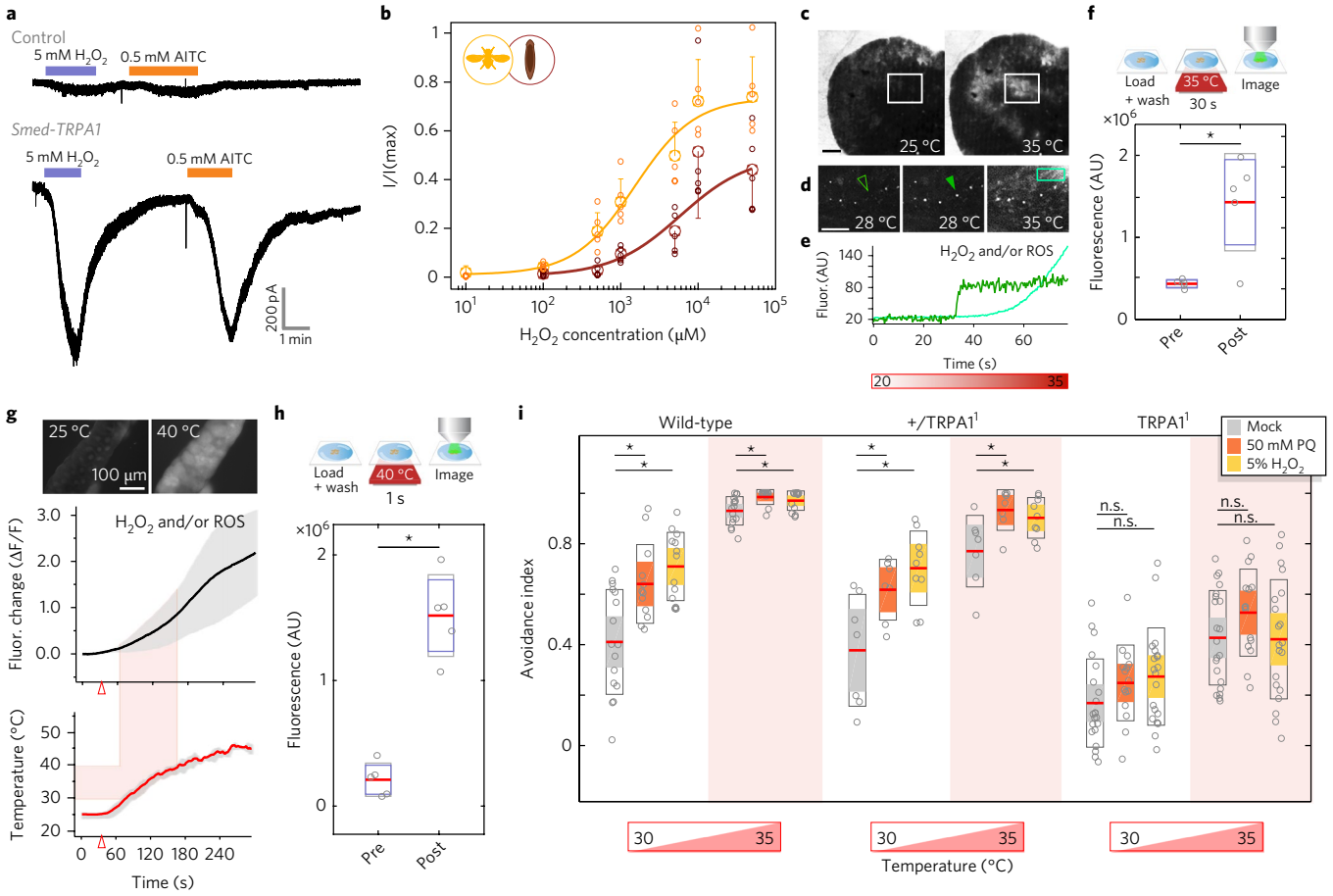

Fig. 6 | H_2O_2 and/or ROS as a signal for TRPA1 activation during noxious heat responses. a, Heterologously expressed *Smed-TRPA1* is activated by H_2O_2. **b**, Dose-response graph of H_2O_2 activation for *Drosophila* TRPA1-C (yellow) and Smed-TRPA1 (brown; mean ± s.d., $n = 5$ cells per condition). **c**–**e**, The ROS dye carboxy-H_2DCFDA demonstrates in vivo ROS production in response to heat in living planarians. **c**,**d**, Representative frames of tissues and cells undergoing rapid fluorescent changes in response to heat. The box in (**c**) highlights a region of the animal in which the increase in fluorescence is particularly obvious. Scale bars in **c** and **d**, 200 μm. **e**, Traces are from an ROI around the cell in **d** (arrow) and the light-green box. **f**, Exposure of planarian worms to 35 °C for 30 s results in a significant increase in fluorescence (unpaired *t* test, $*P = 0.003$, $t_8 = 4.1258$; $n = 5$ worms per condition). Pre, before temperature treatment; Post, after temperature treatment. **g**, Carboxy-H_2DCFDA fluorescence in response to heating in *Drosophila* salivary gland tissue (mean ± s.d.; $n = 5$ salivary glands per condition, from 5 animals). **h**, Exposure of salivary glands to 40 °C for 1 s results in a significant fluorescence increase (unpaired *t* test, $*P = 3.26 \times 10^{-5}$, $t_8 = 8.3283$; $n = 5$ salivary glands per condition, from 5 animals). **i**, Acute feeding with pro-oxidants sensitizes adult *Drosophila* to heat. Feeding paraquat (PQ; orange) or H_2O_2 (yellow) results in increased heat avoidance in a two-choice behavioral assay in both wild-type and heterozygous TRPA1/+ controls (unpaired *t* tests; from left: $*P = 0.003$, $t_{26} = 3.2093$, $n = 16$ groups of ~20 wild-type flies and 12 groups of ~20 TRPA1/+ controls; $*P = 1.26 \times 10^{-4}$, $t_{27} = 4.472$, $n = 16$ wild-type and 13 TRPA1/+ flies; $*P = 0.005$, $t_{26} = 3.058$, $n = 16$ wild-type and 12 TRPA1/+ flies; $*P = 0.036$, $t_{27} = 2.201$, $n = 16$ wild-type and 13 TRPA1/+ flies; $*P = 0.027$, $t_{12} = -2.51$, $n = 7$ wild-type and 7 TRPA1/+ flies; $*P = 0.003$, $t_{14} = -3.53$, $n = 7$ wild-type and 9 TRPA1/+ flies; $*P = 0.021$, $t_{12} = -2.64$, $n = 7$ wild-type and 7 TRPA1/+ flies; $*P = 0.033$, $t_{14} = -2.35$, $n = 7$ wild-type and 9 TRPA1/+ flies). In contrast, heat avoidance does not increase in TRPA1 mutants (n.s., not significant in unpaired *t* tests; from left: $*P = 0.16$, $t_{34} = -1.43$, $n = 21$ wild-type and 15 TRPA1/+ flies; $*P = 0.075$, $t_{39} = -1.82$, $n = 21$ wild-type and 20 TRPA1/+ flies; $*P = 0.11$, $t_{34} = -1.62$, $n = 21$ wild-type and 15 TRPA1/+ flies; $*P = 0.93$, $t_{39} = 0.088$, $n = 21$ wild-type and 20 TRPA/+ flies). In (**f**), (**h**), and (**i**): line, mean; outer boxes, ±1 s.d.; inner boxes, 95% confidence interval).

Next, we tested whether heat stimulation in the appropriate range (i.e., in the noxious range for each species) may lead to the rapid production of H_2O_2 and/or ROS in both *Schmidtea* and *Drosophila* tissues. For this experiment, we loaded living samples with the dye 5-(and 6)-carboxy-2',7'-dichlorodihydrofluorescein diacetate (carboxy-H_2DCFDA, a widely used fluorogenic ROS marker for live cells[44]) and monitored potential fluorescence changes in response to heat exposure by confocal microscopy. As previously reported, live planarian worms could be directly loaded with the dye, and they displayed ROS-induced fluorescence at sites of physical wounding[35] (data not shown; see Supplementary Fig. 3 for additional controls). Fast ROS production was also detected when the worms were submitted to rapid heating while under the microscope (i.e., by using a heating stage; $\Delta t = 20° > 35$ °C, at ~0.25 °C per s). Consistent with the noxious range for this animal (30–35 °C), we observed rapid ROS increases starting above 23–25 °C and culminating in widespread fluorescence around 30–35 °C (Fig. 6c–e). *Drosophila* tissues also displayed rapid ROS increases in response to heating, but this time the increase in fluorescence started around 30 °C and culminated around 40–45 °C (Fig. 6f,g), consistent with the noxious range for *Drosophila* (35–40 °C). Notably, in both planarians and fly tissues, we recorded fluorescence changes rapid enough to be compatible with the timescale that would be required to trigger and/or modulate behavioral responses: for example, between two imaging frames (i.e., separated by ~350 ms; Fig. 6d) or after as little as 1 s of exposure to heat (Fig. 6h).

Carboxy-H_2DCFDA is a general oxidative stress indicator and does not discriminate amongst different reactive oxygen species. To directly test whether H_2O_2 in particular may be amongst the species produced during a noxious heat challenge, we turned to the genetically encoded H_2O_2 indicator roGFP2-Orp1. This indicator couples the redox-sensitive green fluorescent protein 2 (roGFP2) with the yeast H_2O_2 sensor Orp1, allowing the measurement of changes in H_2O_2 levels in intact, living tissues[45]. Our results show that, in transgenic *Drosophila* larvae, roGFP2-Orp1 reported a significant increase in H_2O_2 upon brief (~5 s) exposure to noxious heat (Supplementary Fig. 4; and see Methods for details).

Finally, we tested the notion that, if noxious temperatures are indeed sensed at least in part through H_2O_2 and/or ROS production, an acute, systemic increase in H_2O_2 and/or ROS levels may sensitize the animal's behavioral responses to heat. Here we tested adult *Drosophila* for heat avoidance using our two-choice assay (see above), but this time the flies' performance in the arena was preceded by a short feeding with H_2O_2 or paraquat (a potent pro-oxidant[46]). Strikingly, pro-oxidant feeding significantly increased heat avoidance scores in both wild-type and control flies (to both 30° and 35 °C) but not in TRPA1-mutant flies (Fig. 6i). This result directly demonstrates that H_2O_2 and/or ROS can sensitize aversive responses to heat in *Drosophila* and that this sensitization requires functional TRPA1 channels.

Is TRPA1 also involved in mechanical nociception in *Schmidtea*, as it is in flies[10] and mice[47]? In planarians (as well as in vertebrates[33] and *Drosophila*[34]) H_2O_2 is produced at the site of wounding[35]; therefore, our results predict that TRPA1 signaling should also be activated by mechanical injury in *Schmidtea*. Immediately following physical damage (i.e., when cut), planarian worms engage in a behavior called 'scrunching'[48], an unusual escape gait that persists for ~15 s after the immediate injury. Indeed, scrunching following physical injury was reduced in planarians in which *Smed-TRPA1* was knocked down by RNAi (Supplementary Fig. 5). This result supports the notion that Smed-TRPA1 may also be involved in mechanical nociception and suggests a model in which either thermal or mechanical injury can activate Smed-TRPA1 through H_2O_2 and/or ROS production.

Discussion

Planarian flatworms are a powerful yet underutilized model for behavioral research. They are capable of active hunting behavior and possess simple sensory systems[27,49] and a simple brain that operates using synaptic and neurotransmitter principles similar to those of the more complex insect or mammalian brains[50]. Here we have shown that the ion channel TRPA1 functions as a key transduction component for nociceptive signals in *S. mediterranea*. In insects and many vertebrates (snakes, frogs, etc.), TRPA1 channels can be directly gated by temperature changes, but our work in *Schmidtea* and *Drosophila* suggests that TRPA1's function in nociceptive heat sensing goes beyond that of a canonical heat-activated ion channel. Instead, our data suggest that H_2O_2 and/or ROS are rapidly produced in response to noxious heat and that this signal contributes to channel activation to mediate defensive responses. We note that this mechanism provides an especially satisfactory explanation for the remarkable across-phylum rescue of heat-avoidance phenotypes of TRPA1 mutant *Drosophila* by both *Schmidtea* TRPA1 (insensitive to heat), as well as by human TRPA1 (activated by cold). The heat range that is expected to produce tissue damage in *Drosophila* (i.e., the noxious range, ~35–40 °C) is different from that of *Schmidtea* (~30 °C) and from that of humans (~45 °C), yet transgenic rescue of fly mutants restored heat avoidance to that of the host (*Drosophila*) rather than the channel donor (*Schmidtea* or human). This can be accounted for by the fact that the thermal range that causes heat damage (and therefore H_2O_2 and/or ROS production) is determined by the heat tolerance of the host tissue.

Finally, our results suggest that early Bilaterians already possessed a polymodal (thermal–mechanical–chemical) nociceptive system that relied on H_2O_2- and/or ROS-mediated TRPA1 activation. This core function has been conserved in extant lineages and may have placed TRPA1 in a key position to undergo the additional transitions into the hot- or cold-activated channels that have been documented in various animal groups. Our results also imply that human pain systems may share a common ancestry with the nociceptive systems of extant bilateral animals, tracing back their origin to the common 'urbilaterian' progenitor, which lived more than 500 million years ago.

Methods

Methods, including statements of data availability and any associated accession codes and references, are available at https://doi.org/10.1038/s41593-017-0005-0.

Received: 19 June 2017; Accepted: 6 September 2017;
Published online: 16 October 2017

References

1. Kremeyer, B. et al. A gain-of-function mutation in *TRPA1* causes familial episodic pain syndrome. *Neuron* **66**, 671–680 (2010).
2. Viswanath, V. et al. Opposite thermosensor in fruitfly and mouse. *Nature* **423**, 822–823 (2003).
3. Jordt, S. E. et al. Mustard oils and cannabinoids excite sensory nerve fibres through the TRP channel ANKTM1. *Nature* **427**, 260–265 (2004).
4. Bandell, M. et al. Noxious cold ion channel TRPA1 is activated by pungent compounds and bradykinin. *Neuron* **41**, 849–857 (2004).
5. Macpherson, L. J. et al. The pungency of garlic: activation of TRPA1 and TRPV1 in response to allicin. *Curr. Biol.* **15**, 929–934 (2005).
6. Bautista, D. M. et al. Pungent products from garlic activate the sensory ion channel TRPA1. *Proc. Natl. Acad. Sci. USA* **102**, 12248–12252 (2005).
7. Bautista, D. M. et al. TRPA1 mediates the inflammatory actions of environmental irritants and proalgesic agents. *Cell* **124**, 1269–1282 (2006).
8. Macpherson, L. J. et al. An ion channel essential for sensing chemical damage. *J. Neurosci.* **27**, 11412–11415 (2007).
9. Neely, G. G. et al. TrpA1 regulates thermal nociception in Drosophila. *PLoS One* **6**, e24343 (2011).
10. Zhong, L. et al. Thermosensory and nonthermosensory isoforms of *Drosophila melanogaster* TRPA1 reveal heat-sensor domains of a thermoTRP channel. *Cell Reports* **1**, 43–55 (2012).
11. Kang, K. et al. Analysis of Drosophila TRPA1 reveals an ancient origin for human chemical nociception. *Nature* **464**, 597–600 (2010).
12. Chatzigeorgiou, M. et al. Specific roles for DEG/ENaC and TRP channels in touch and thermosensation in *C. elegans* nociceptors. *Nat. Neurosci.* **13**, 861–868 (2010).
13. Laursen, W. J., Bagriantsev, S. N. & Gracheva, E. O. TRPA1 channels: chemical and temperature sensitivity. *Curr. Top. Membr.* **74**, 89–112 (2014).
14. Chen, J. et al. Species differences and molecular determinant of TRPA1 cold sensitivity. *Nat. Commun.* **4**, 2501 (2013).
15. Saito, S. et al. Heat and noxious chemical sensor, chicken TRPA1, as a target of bird repellents and identification of its structural determinants by multispecies functional comparison. *Mol. Biol. Evol.* **31**, 708–722 (2014).
16. Gracheva, E. O. et al. Molecular basis of infrared detection by snakes. *Nature* **464**, 1006–1011 (2010).
17. Saito, S. et al. Analysis of transient receptor potential ankyrin 1 (TRPA1) in frogs and lizards illuminates both nociceptive heat and chemical sensitivities and coexpression with TRP vanilloid 1 (TRPV1) in ancestral vertebrates. *J. Biol. Chem.* **287**, 30743–30754 (2012).
18. Oda, M., Kurogi, M., Kubo, Y. & Saitoh, O. Sensitivities of two zebrafish TRPA1 paralogs to chemical and thermal stimuli analyzed in heterologous expression systems. *Chem. Senses* **41**, 261–272 (2016).
19. Prober, D. A. et al. Zebrafish TRPA1 channels are required for chemosensation but not for thermosensation or mechanosensory hair cell function. *J. Neurosci.* **28**, 10102–10110 (2008).
20. Kohno, K., Sokabe, T., Tominaga, M. & Kadowaki, T. Honey bee thermal/chemical sensor, AmHsTRPA, reveals neofunctionalization and loss of transient receptor potential channel genes. *J. Neurosci.* **30**, 12219–12229 (2010).
21. Wang, G. et al. *Anopheles gambiae* TRPA1 is a heat-activated channel expressed in thermosensitive sensilla of female antennae. *Eur. J. Neurosci.* **30**, 967–974 (2009).
22. Kang, K. et al. Modulation of TRPA1 thermal sensitivity enables sensory discrimination in Drosophila. *Nature* **481**, 76–80 (2011).

23. Dunn, C. W., Giribet, G., Edgecombe, G. D. & Hejnol, A. Animal phylogeny and its evolutionary implications. *Annu. Rev. Ecol. Evol. Syst.* **45**, 371–395 (2014).
24. Newmark, P. A., Reddien, P. W., Cebrià, F. & Sánchez Alvarado, A. Ingestion of bacterially expressed double-stranded RNA inhibits gene expression in planarians. *Proc. Natl. Acad. Sci. USA* **100** (Suppl. 1), 11861–11865 (2003).
25. Wenemoser, D., Lapan, S. W., Wilkinson, A. W., Bell, G. W. & Reddien, P. W. A molecular wound response program associated with regeneration initiation in planarians. *Genes Dev.* **26**, 988–1002 (2012).
26. Gallio, M., Ofstad, T. A., Macpherson, L. J., Wang, J. W. & Zuker, C. S. The coding of temperature in the Drosophila brain. *Cell* **144**, 614–624 (2011).
27. Inoue, T., Yamashita, T. & Agata, K. Thermosensory signaling by TRPM is processed by brain serotonergic neurons to produce planarian thermotaxis. *J. Neurosci.* **34**, 15701–15714 (2014).
28. Wang, H., Schupp, M., Zurborg, S. & Heppenstall, P. A. Residues in the pore region of Drosophila transient receptor potential A1 dictate sensitivity to thermal stimuli. *J. Physiol. (Lond.)* **591**, 185–201 (2013).
29. Cordero-Morales, J. F., Gracheva, E. O. & Julius, D. Cytoplasmic ankyrin repeats of transient receptor potential A1 (TRPA1) dictate sensitivity to thermal and chemical stimuli. *Proc. Natl. Acad. Sci. USA* **108**, E1184–E1191 (2011).
30. Kwon, Y., Shim, H.-S., Wang, X. & Montell, C. Control of thermotactic behavior via coupling of a TRP channel to a phospholipase C signaling cascade. *Nat. Neurosci.* **11**, 871–873 (2008).
31. Lee, Y. & Montell, C. Drosophila TRPA1 functions in temperature control of circadian rhythm in pacemaker neurons. *J. Neurosci.* **33**, 6716–6725 (2013).
32. Ni, L. et al. A gustatory receptor paralogue controls rapid warmth avoidance in Drosophila. *Nature* **500**, 580–584 (2013).
33. Niethammer, P., Grabher, C., Look, A. T. & Mitchison, T. J. A tissue-scale gradient of hydrogen peroxide mediates rapid wound detection in zebrafish. *Nature* **459**, 996–999 (2009).
34. Moreira, S., Stramer, B., Evans, I., Wood, W. & Martin, P. Prioritization of competing damage and developmental signals by migrating macrophages in the Drosophila embryo. *Curr. Biol.* **20**, 464–470 (2010).
35. Pirotte, N. et al. Reactive oxygen species in planarian regeneration: an upstream necessity for correct patterning and brain formation. *Oxid. Med. Cell. Longev.* **2015**, 392476 (2015).
36. Xu, C., Luo, J., He, L., Montell, C. & Perrimon, N. Oxidative stress induces stem cell proliferation via TRPA1/RyR-mediated Ca(2+) signaling in the Drosophila midgut. *eLife* **6**, e22441 (2017).
37. Andersson, D. A., Gentry, C., Moss, S. & Bevan, S. Transient receptor potential A1 is a sensory receptor for multiple products of oxidative stress. *J. Neurosci.* **28**, 2485–2494 (2008).
38. Du, E. J. et al. Nucleophile sensitivity of Drosophila TRPA1 underlies light-induced feeding deterrence. *eLife* **5**, e18425 (2016).
39. Guntur, A. R. et al. H2O2-sensitive isoforms of *Drosophila melanogaster* TRPA1 act in bitter-sensing gustatory neurons to promote avoidance of UV during egg-laying. *Genetics* **205**, 749–759 (2017).
40. Guntur, A. R. et al. Drosophila TRPA1 isoforms detect UV light via photochemical production of H2O2. *Proc. Natl. Acad. Sci. USA* **112**, E5753–E5761 (2015).
41. Kim, M. J. & Johnson, W. A. ROS-mediated activation of Drosophila larval nociceptor neurons by UVC irradiation. *BMC Neurosci.* **15**, 14 (2014).
42. Birkholz, T. R. & Beane, W. S. The planarian TRPA1 homolog mediates extraocular behavioral responses to near-ultraviolet light. *J. Exp. Biol.* **220**, 2616–2625 (2017).
43. Miyake, T. et al. Cold sensitivity of TRPA1 is unveiled by the prolyl hydroxylation blockade-induced sensitization to ROS. *Nat. Commun.* **7**, 12840 (2016).
44. Kalyanaraman, B. et al. Measuring reactive oxygen and nitrogen species with fluorescent probes: challenges and limitations. *Free Radic. Biol. Med.* **52**, 1–6 (2012).
45. Albrecht, S. C., Barata, A. G., Grosshans, J., Teleman, A. A. & Dick, T. P. In vivo mapping of hydrogen peroxide and oxidized glutathione reveals chemical and regional specificity of redox homeostasis. *Cell Metab.* **14**, 819–829 (2011).
46. Rzezniczak, T. Z., Douglas, L. A., Watterson, J. H. & Merritt, T. J. Paraquat administration in Drosophila for use in metabolic studies of oxidative stress. *Anal. Biochem.* **419**, 345–347 (2011).
47. Kwan, K. Y. et al. TRPA1 contributes to cold, mechanical, and chemical nociception but is not essential for hair-cell transduction. *Neuron* **50**, 277–289 (2006).
48. Cochet-Escartin, O., Mickolajczyk, K. J. & Collins, E. M. Scrunching: a novel escape gait in planarians. *Phys. Biol.* **12**, 056010 (2015).
49. Inoue, T., Hoshino, H., Yamashita, T., Shimoyama, S. & Agata, K. Planarian shows decision-making behavior in response to multiple stimuli by integrative brain function. *Zoological letters* **1**, 7 (2015).
50. Umesono, Y., Tasaki, J., Nishimura, K., Inoue, T. & Agata, K. Regeneration in an evolutionarily primitive brain-the planarian *Dugesia japonica* model. *Eur. J. Neurosci.* **34**, 863–869 (2011).

Acknowledgements

We thank D. Tracey and R. Carthew for reagents; A. Kuang and L. Vinson for technical assistance; L. Macpherson, D. Yarmolinsky, and members of the Gallio Lab for comments on the manuscript; I. Raman for technical advice, and M. Stensmyr for the kind gift of the fly drawing in Fig. 1. Work in the Gallio lab is supported by NIH grant R01NS086859 (to M.G.), the Chicago Biomedical Consortium with support from the Searle Funds at the Chicago Community Trust (to E.E.Z.), and by training grant 2T32MH067564 (to O.M.A.). Work in the Petersen Lab is supported by an NIH Director's New Innovator award (1DP2DE024365-01).

Author contributions

M.G. designed the study, analyzed the data, and wrote the paper with critical input from all authors; M.G. and O.M.A. designed and built the behavioral assays. O.M.A. performed all planarian behavioral experiments and electrophysiology and analyzed the corresponding data. E.E.Z. performed all fly rescue experiments and ROS assays and analyzed the corresponding data. A.P. cloned *Smed-TRPA1*, produced rescue constructs and transgenics, and analyzed sequences with help from C.P.P.; A.P., O.M.A., and C.V.D. performed q-PCR and ISH experiments. E.E.Z. and O.M.A. generated human-TRPA1-expressing flies.

Competing interests

The authors declare no competing financial interests.

Additional information

Supplementary information is available for this paper at https://doi.org/10.1038/s41593-017-0005-0.

Reprints and permissions information is available at www.nature.com/reprints.

Correspondence and requests for materials should be addressed to M.G.

Publisher's note: Springer Nature remains neutral with regard to jurisdictional claims in published maps and institutional affiliations.

Methods

Cloning of a *Smed-TRPA1* full-length coding sequence. A full-length *Smed-TRPA1* coding sequence was amplified by PCR starting from an *S. mediterranea* cDNA library. The library was generated by Superscript III reverse transcription (Life Technologies) from total RNA, purified from whole animals using Trizol followed by DNAse treatment with DNA-free (Ambion/ThermoFisher). The following primers were used for PCR: FWD 5′-CAaaacATGAATAAAATTTCTAAAAACCGAAAAACCTC-3′ and REV 5′-TTAAAAATTGTTATCTGGTTTGACAGATTTCTG-3′ (Kozak sequence for Drosophila in lower case letters). Analysis of 5′- and 3′- RACE libraries produced with SMARTer RACE 5′/3′ Kit (Clontech) confirmed that the identified sequence included the appropriate ATG and stop codons and represented a single, full-length *Smed-TRPA1* coding sequence (3,510 bp). Analysis of available RNAseq data (SmedGD, http://smedgd.neuro.utah.edu/)[51] indicates that *Smed-TRPA1* likely produces a single transcript, encoding a protein of 1,169 amino acids that contains 14 N-terminal ankyrin repeats (Interpro: IPR002110) followed by an ion transporter domain (Interpro: IPR005821).

Phylogenetic analysis of TRPA1 homologs. A neighbor-joining phylogenetic tree was constructed using the full sequence of bona fide (experimentally validated) TRPA1 proteins from 24 organisms: *A. gambiae* (ACC86138), *A. aegypti* (AAEL009419), *D. melanogaster* (AEU17952), *B. mori* (NP_001296525), *C. elegans* (ABQ15208), *C. brevicauda* (AEL30802), *C. porcellus* (NP_001185699), *C. hortulanus* (ADD82932), *C. atrox* (ADD82930), *D. rerio* (NP_001007066 and NP_001007067), *D. rotundus* (AEL30803), *G. gallus* (NP_001305389), *H. armigera* (AHV83756), *H. sapiens* (NP_015628), *M. mulatta* (XP_001083172), *M. musculus* (NP_808449), *P. obsoletus lindheimeri* (ADD82929), *P. jerdonii* (AEW26660), *P. regius* (ADD82928), *R. norvegicus* (NP_997491), *T. rubripes* (XP_003968031), *T. castaneum* (LOC658860), *V. destructor* (BAO73033 and BAO73034), and *X. tropicalis* (BAM42680).

Planarian RNAi. The CIW4 asexual laboratory strain of *S. mediterranea* was used for all experiments. Animals were kept in plastic containers filled with 1× artificial planarian water (APW) that contained 1.6 mM NaCl, 1 mM $CaCl_2$, 1 mM $MgSO_4$, 0.1 mM $MgCl_2$, 0.1 mM KCl, and 1.2 mM $NaHCO_3$. Planarians were fed homogenized calf liver for stock maintenance. The containers were cleaned 2 d after feeding or once a week if starved. Templates for RNA synthesis were generated by PCR from pGEM-t vectors (Promega) harboring 1.5-kb fragments of *Smed-TRPA1* or *Smed-AP2* cDNA; a 0.8-kb *UNC22* PCR product was used to generate *UNC22* template as an RNAi control (*UNC22* is a *C. elegans* gene not present in the *S. mediterranea* genome). The T7 RNA polymerase promoter was introduced to the 5′ end or 3′ end of the corresponding fragment, and two subsequent PCR reactions were performed to generate sense and antisense RNA strands. Sense and antisense strands were pooled together, purified by phenol-chloroform extraction, and resuspended in 16 µL of water before being annealed by incubating at 72 °C, then 37 °C, and finally on ice. dsRNA was mixed with 80 µL of homogenized calf liver and 2 µL of red food coloring to assess food intake. Planarians were starved for at least a week and then fed the dsRNA every other day 3–4 times (15 µL of food for 10–15 animals). Animals that did not feed were discarded. For behavioral experiments, animals were used between 1 d and 4 d after their last feeding; phototaxis was used at the end of each experiment to ensure viability.

Expression analysis by q-PCR. Total RNA from *UNC22*, *Smed-AP2,* and *Smed-TRPA1*-knockdown planarians was purified using a Trizol reagent (Life Technologies). First-strand cDNA was synthesized using MultiScribe Reverse Transcriptase (Fisher Scientific) from DNAse-treated (TURBO DNAse, Ambion) total RNA. Q-PCR reactions were performed using the EvaGreen dye (Biotium). Four biological replicates were run for each treatment, with *clathrin* mRNA detected as reference gene for quantifying expression changes using the ΔΔCt method and normalizing to the expression obtained in the control RNAi treatment. *Smed-TRPA1* was detected using the primers 5′-ACTCTCATCAACAGACAGA CTTGT3′ and 5′-ATTTCAGCCTCTGGATCCATTTCC-3′; *clathrin* primers were 5′-GACTGCGGGCTTCTATTGAG-3′ and 5′-GCGGCAATTCTTCTGAACTC-3′. Results were compared using Kruskal-Wallis tests.

Fluorescent in situ hybridization (FISH). *Smed-TRPA1* riboprobes were generated from a PCR fragment flanked by T7 promoter sequences using RNA DIG-labeling mix (Sigma-Aldrich). After in vitro transcription, antisense probes were precipitated with 100% ethanol and resuspended in 25 µL of deionized formamide. Planarians were killed in 5% N-acetyl cysteine and fixed in 4% formaldehyde, followed by dehydration and overnight bleaching in 6% H_2O_2 on a light box. Animals were preserved in 100% methanol and stored at −20 °C. For FISH, planarians were rehydrated with a methanol:PBST (PBS, 0.1% Triton X-100) dilution series; next, animals were treated with 10 mg/mL proteinase K, postfixed in 4% formaldehyde, and incubated at 56 °C for 2 h in prehybridization solution (50% of deionized formamide, 5× SSC, 0.1 mg/mL yeast RNA, 1% Tween-20 in DEPC-treated water). Hybridization with riboprobes was conducted for 16 h in hybridization solution (prehybridization solution plus 5% dextran sulfate). Then animals were washed in prehybridization solution and subjected to a dilution series of 2× SSC, then 0.2× SSC, and finally TNTx (0.1 M Tris pH 7.5, 0.15 M NaCl, 0.3% Triton X-100). Animals were blocked in TNTx plus 5% horse serum and 5% western blocking reagent (Sigma-Aldrich) for 2 h at RT, and then labeled with a sheep anti-DIG-POD antibody (1:2,000, Sigma-Aldrich #11207733910) in blocking solution overnight at 4 °C. Animals were washed 8× in TNTx, incubated in tyramide solution with rhodamine (1:500) and H_2O_2 for 10 minutes with shaking. Finally, animals were rinsed 6× in TNTx. ISH experiments were performed four times with similar results. To quantify $TRPA1^+$ cells in various groups (Fig. 1f–k), ten worms per treatment were imaged with a Leica DM 2500 confocal microscope with a 10× objective and 1.5 digital zoom, and *z*-stacks encompassing the thickness of each animal were acquired at 5-µm intervals, using constant laser and PMT settings. *Z*-stacks were analyzed using ImageJ: brightness/contrast was adjusted in batch using identical settings and max projection images through the animal were produced. From these, the number of fluorescent cells in a defined ROI in the brain region and a defined ROI at the periphery (each of constant size, shown as yellow boxes in Fig. 1) were counted. The numbers of fluorescent cells were then plotted and compared by unpaired *t* test.

Planarian behavioral assays: heat avoidance. Heat avoidance was measured in the 'Planariometer' (Supplementary Fig. 1). The Planariometer consisted of four independent tiles covered by thin anodized aluminum foil. A hydrophobic ink pen (Super PAP pen; ThermoFisher) was used to create a circular barrier (55 mm in diameter) to allow a thin film of water (1–2 mm) to form a central pool in which the worms can move freely. In each experiment, two opposite tiles were set at 32 °C and two at 24 °C, and animal movement was recorded for 4 min. The spatial configuration of hot and cool tiles was then reversed for an additional 4 min (and a second video recorded) to control for potential spatial biases. Experiments were conducted in the dark with infrared (IR) LED illumination, and videos were recorded with an IR-sensitive CCD camera (Basler). Five independent groups of ten animals per treatment were used. The heat avoidance index (AI = (number of worms at 24 °C – number of worms at 32 °C)/total number of worms) was calculated from the last 120 frames of each video (last 1 min of the video) by measuring the positions of the worms every three frames using standard Matlab scripts. Avoidance index values were compared using Kruskal-Wallis tests followed by Tukey's honest significant difference tests.

Planarian behavioral assays: AITC avoidance. Five independent groups of 10 animals per treatment were tested in an arena composed of two circular chambers connected by a narrow corridor. At the beginning of the experiment, all animals were placed in chamber 1, together with a small block of control agar (1% agarose dissolved in 1× APW) or AITC-laced agar. The AITC-laced agar was made with 1% agarose in 1× APW and 50 mM AITC. The chamber was placed in the dark, animals were illuminated with IR light and their behavior was recorded for 5 min with an IR-sensitive CCD camera. Videos were analyzed, and the number of planarians in each chamber was quantified every 10 frames for the last 125 frames of the video (last minute). The fraction of animals in each chamber was counted after each treatment and compared using Kruskal-Wallis tests followed by Tukey's honest significant difference test. Image analysis was performed using Matlab.

Planarian behavioral assays: negative phototaxis. Four independent groups of 10 worms per treatment were placed in chamber 1 of the arena as described above (AITC avoidance experiments). The arena was either kept completely dark (control condition); alternatively, chamber 1 was exposed to bright light while chamber 2 was kept dark. Animals were allowed to explore freely for 2 min before the number of worms in each chamber was counted.

Planarian behavioral assays: scrunching. Scrunching behavior was assessed as previously described[48], with modifications. Animals were recorded under a standard dissecting scope equipped with a Pointgrey USB camera. Planarians were placed on wet filter paper and the tail was amputated with a scalpel while recording. Amputation time was set as $t = 0$ and total body area was subsequently measured 3× per s for 15 s. Area measurements were normalized to the mean body area for each animal, averaged across the movie. Average wave amplitude was calculated across the 15-min movie and compared using unpaired *t* tests. Image analysis was performed using Matlab.

Cell transfections. pAC-GFP, pAC-Smed-TRPA1, and pAC-dTRPA1-A were generated by cloning GFP, *Smed-TRPA1* ORF (see above), and a *dTRPA1-A* cDNA (a gift of D. Tracey, Indiana University, Bloomington, Indiana, USA) into pCR 8/GW/TOPO TA (ThermoFisher), and then transferring them into a pAC-GW expression vector (created by ligating the Gateway cassette from pMartini Gate C R2-R1 (Addgene plasmid #36436) cut with XhoI and XbaI into pAc5.1/V5-His A (ThermoFisher)). $S2R^+$ cells (a gift from R. Carthew, Northwestern University, Evanston, IL, USA) were cultured in Schneider's Drosophila Medium (Lonza) supplemented with 10% fetal bovine serum and 1% penicillin–streptomycin mixture (100 units/mL and 100 µg/mL respectively; Fisher Scientific). For electrophysiological recordings, $S2R^+$ cells were grown on coverslips in Schneider's Drosophila Medium supplemented with 50 µM $LaCl_3$ and transfected with 50 ng of pAC-GFP vector and 500 ng of either pAC-dTRPA1-A or pAC-Smed-TRPA1 vectors mixed with 4 µL of enhancer and 150 µL of buffer EC. After 5 min, 6.5 µL of

Effectene Transfection Reagent (Qiagen) was added and the mix was incubated for 10 min before being dispensed to the cells. Transfected cells were incubated at RT for at least 36 h to allow gene expression.

Electrophysiological recordings. Whole-cell voltage-clamp recording was performed on S2R$^+$ transfected cells identified by GFP fluorescence. The intracellular solution contained 140 mM methanesulfonic acid, 2 mM $MgCl_2$, 1 mM EGTA, 5 mM HEPES, and 1 mM Na_2ATP; pH was adjusted to 7.3 with CsOH and the osmolarity was adjusted to 315 ± 5 mOsml with sucrose. The extracellular solution contained 140 mM NaCl, 5 mM KCl, 1 mM $CaCl_2$, 1 mM HEPES, and 10 mM glucose; pH was adjusted to 7.2 with NaOH and the osmolarity was adjusted to 310 ± 5 mOsml with sucrose. Patch pipettes resistance ranged from 5 to 10 MΩ. Recordings were obtained with an AxoPatch 200b amplifier (Axon Instruments) and analyzed with AxoGraph software and Matlab scripts. Recordings were made with 1× output gain and a 5-kHz low-pass filter. Bath offsets and capacitance were compensated for; series resistance was 9.5 ± 5.5 MΩ without compensation. Recordings were made at RT (22–23 °C) and temperature stimulation was achieved by raising the temperature of the bath solution via an inline heater (HPT-2A, ALA Scientific Instruments) and a TC-20 temperature controller (NPI Electronics). Temperature was monitored with a T-384 thermocouple (Physitemp Instruments) tethered to the electrode holder, so that the tip of the thermocouple was at an approximately constant distance from the tip of the recording electrode (1–2 mm). Chemical stimulation was achieved by bath perfusion of extracellular solution containing 500 µM of allyl isothiocyanate (AITC, Sigma). Cells were held at −60 mV and currents were monitored during heat and chemical stimulation. Current–voltage relationships were constructed by averaging three voltage-step protocols consisting of 100-ms steps of 20 mV from −100 to +100 mV, separated by 400 ms. These I–V relationships where made at RT, during the heat stimulation, and at the end of a 3-min AITC application. Note that Smed-TRPA1 did not appear to respond to cooling. For the AITC and hydrogen peroxide dose-responses (H_2O_2, Sigma, 30% w/w) we used 1-min stimulations at each concentration. Recordings were performed as described above, except that the intracellular solution contained 140 mM potassium-gluconate instead of cesium.

Fly strains and transgenes. Flies were reared on standard cornmeal agar medium at room temperature (RT). The following fly strains were used: Canton-special, isogenic w^{1118} (a gift from Marcus C. Stensmyr, Lund University, Lund, Sweden); elav-Gal4/CyO; *trpA1*^{1} (BDSC #26504, backcrossed five times), 5xUAS-TRPA1-C (a gift from D. Tracey, Indiana University, Bloomington, Indiana, USA), and tub-cyto-roGFP2-Orp1[49]. To generate *UAS-SmedTRPA1* flies, *Smed-TRPA1* cDNA (see above) was cloned into pCR 8/GW/TOPO TA (Invitrogen) and then transferred into a 40× UAS destination vector created by introducing the Gateway cassette into pJFRC8-40XUAS- IVS-mCD8::GFP (Addgene #26221) via the XhoI/XbaI restriction sites. This construct was then used for embryo injection by BestGene Inc. to generate P[40XUAS::Smed-TRPA1]attP40 flies. Similarly, *UAS-humanTRPA1* flies were obtained starting from a human TRPA1 cDNA (NP_015628; a gift from M. Hoon, NIDCR/NIH, Bethesda, Maryland, USA) to generate P[40XUAS::hTRPA1] attP40 flies. Expression of the transgenes was confirmed by RT PCR. Full genotypes of fly stocks used in Fig. 5: *w*^{1118}, *w*^{1118}*;TRPA1*^{1}, *w*^{1118}*;elav-Gal4/+;TRPA1*^{1}*/TRPA1*^{1}, *w*^{1118}*;+/UAS-TRPA1-C;TRPA1*^{1}*/TRPA1*^{1}, *w*^{1118}*;elav-Gal4/UAS-TRPA1-C;TRPA1*^{1}*/TRPA1*^{1}, *w*^{1118}*;+/UAS-Smed-TRPA1;TRPA1*^{1}*/TRPA1*^{1}, *w*^{1118}*;elav-Gal4/UAS-Smed-TRPA1;TRPA1*^{1}*/TRPA1*^{1}, *w*^{1118}*;+/UAS-humanTRPA1;TRPA1*^{1}*/TRPA1*^{1}, and *w*^{1118}*;elav-Gal4/UAS-human TRPA1;TRPA1*^{1}*/TRPA1*^{1}.

Drosophila behavioral assays. Temperature preference assay were performed as previously described[26]. In brief, avoidance index (AI) values for the test temperatures (TT) are calculated as follows: AI = (number of flies at 25 °C – number of flies at TT)/(total number of flies). AI values were compared using ANOVA or two-way ANOVA as previously described. Avoidance index values for experiments with Gal4 and UAS lines were compared by two-way ANOVA (threshold $P = 0.01$). Kolmogorov-Smirnov tests were used to test for a normally distributed sample. Homogeneity of variance for each dataset was confirmed by calculating the Spearman correlation between the absolute values of the residual errors and the observed values of the dependent variable (threshold $P = 0.05$). Statistical analysis was carried out in Matlab. All temperature-preference experiments were performed on 3- to 5-day-old male flies in a custom chamber kept at a constant RH of 40%. Heat and AITC-vapor incapacitation experiments (Fig. 4) were performed as follows: flies of the genotypes elav/+, UAS-Smed-TRPA1/+, UAS-TRPA1-1/+ (negative controls), elav-Gal4>UAS-TRPA1-A (positive control), and elav-Gal4>UAS-Smed-TRPA1(experimental animals) were used to test responses to temperature and AITC. For heat incapacitation, groups of ten flies were collected in empty vials and placed in a 25 °C incubator for at least 1 h before the experiments. Next, the vials were submerged in water (preheated to 35 °C) and kept submerged until the internal air temperature of the tube had been at 35 °C for one minute (as measured by a thermocouple). Following this, the incapacitated flies (i.e., flies that had dropped to the bottom of the tube) were counted. Vials were then placed at RT for an additional 3 min, and the number of incapacitated flies scored every minute to measure recovery. For the exposure to AITC vapors, groups of ten flies of each genotype (see above), were collected in 15-mL tubes for bacterial culture with small holes to allow air flow. These 15-mL culture tubes were placed inside a 50-mL conical tube containing a small piece of filter paper with 1 µL of 2.5-M AITC. Flies were exposed to AITC vapors for 10 min and then transferred to clean vials for recovery. The number of incapacitated animals was recorded every 1 min during AITC exposure and every 5 min during recovery. For the pro-oxidant feeding experiments, groups of twenty 3- to 5-day-old flies of the appropriate genotype were starved for 18 h in vials with a Kim-wipe saturated by water. Flies were then fed for 3 h on Nutri-Fly Instant Medium (Genesee Scientific #66-117) prepared with the respective pro-oxidant solution at a ratio of medium to liquid of 1:3. The liquid used contained either the pro-oxidant and sucrose or sucrose alone ('mock'). Final concentrations: all samples = 2% sucrose; H_2O_2 = 5%, paraquat (Sigma #856177) = 50 mM. Immediately after feeding, the animals were tested for temperature preference as described above. Food intake was monitored in parallel experiments using green food colorant (25 µL for 3 mL of solution).

ROS imaging. To evaluate ROS levels in response to heat stimuli in intact live planarians and *Drosophila* tissues, we used the fluorogenic oxidative stress indicator carboxy-H_2DCFDA (Molecular Probes #I36007) per the manufacturer's guidelines (and see below). ROS levels were imaged on an LSM510 Zeiss confocal microscope equipped using a 488-nm argon laser. Temperature stimuli were generated with a Model 5000 KT stage controller (20/20 Technology), and the temperature was recorded using an NI USB-TC01 equipped with a thermocouple probe (National Instruments). Intact planarians were incubated for 1 h in 25 µM carboxy-H_2DCFDA (diluted in APW) and washed briefly in APW prior to imaging. To minimize movements during scanning, animals were placed into a tight-fitting custom-made Sylgard frame mounted on a glass slide and filled with APW. The preparation was sealed with a cover slip. For real time ROS detection, planarians were imaged continuously with a 5× / 0.16 Zeiss air objective at 256 × 256-pixel resolution and 2× optical zoom at 0.395-ms framerate during a heat ramp of $\Delta t = 20\,°C > 35\,°C$, speed = ~1 °C/4 s. ROS-induced fluorescence was measured from confocal images acquired at low resolution and using a fully open pinhole, from ROIs corresponding to large parts of the head region (512 × 512-pixel resolution, 1× optical zoom with a 5× Zeiss air objective). Drosophila salivary glands were dissected in PBS and incubated with 25 µM carboxy-H_2DCFDA (diluted in PBS) for 1 h at room temperature prior to heat stimulation. Tissues were then briefly washed in PBS and transferred into a custom-made thin Sylgard frame containing PBS and mounted on a glass slide. The preparation was sealed with a cover slip. Differences in fluorescence were evaluated using unpaired *t* tests. For real-time ROS detection in *Drosophila*, salivary glands were imaged continuously with a 10× Zeiss air objective at 256 × 256-pixel resolution and 2× optical zoom at 0.395-ms frame-rate during a heat ramp of $\Delta t = 20\,°C > 45\,°C$, speed = ~1 °C/4 s. $\Delta F/F$ analysis was carried out using Matlab scripts, and base fluorescence was calculated using all frames preceding the temperature trigger (occurring at 30 s). Confocal stacks of about 100 µm at 5-µm steps were obtained at 512 × 512-pixel resolution, 1× optical zoom with a 10× Zeiss air objective.

For in vivo H_2O_2 detection in intact animals, tub-cyto-roGFP2-Orp1 larvae were placed on a heated surface set to ~35 °C for 5 s. As a positive control, larvae were exposed to 25 µM H_2O_2 for 10 min. Animals were rapidly dissected after treatment in PBS to extract their wing imaginal discs (as described in ref. [45]). The tissues were mounted in glycerol and immediately imaged on a Leica SP5 inverted confocal microscope equipped with a 405-nm UV laser, a 488-nm argon laser, and a 10× air objective at 512 × 512-pixel resolution and 400 Hz. Image acquisition and processing were performed as above. We used two-sample *t* tests to calculate significant differences ($P < 0.05$) between treatments and controls. Excitations of the biosensor fluorescence by the 405-nm and 488-nm laser lines were performed sequentially and stack by stack. Emission was detected at 500–570 nm. Image processing was performed with ImageJ. Control fluorescence (i.e., of untreated tissue) was set to 1.

Statistics. No statistical methods were used to predetermine sample size. Sample sizes were chosen following accepted standards in the field. No randomization was used. Data collection and analysis were not performed blind to the conditions of the experiments. No animals or data points were excluded from the analyses. Statistical testing was performed in Matlab. Normal data distribution was assessed by Kolmogorov-Smirnov tests. If normality was met, we used unpaired Student's *t* tests and two-way ANOVA for single and multiple comparisons, respectively. If normality was not met, we used Kruskal-Wallis tests. Data graphs were processed using the notBoxPlot Matlab function (kindly provided to the community by R. Campbell, Biozentrum, University of Basel, Basel, Switzerland).
A Life Sciences Reporting Summary is available online.

Accession codes. GenBank: MF818036.

Data and code availability. The data that support the findings of this study are available from the corresponding author upon reasonable request. Our analysis uses standard Matlab functions (image analysis and statistics toolboxes).

References

51. Robb, S. M. C., Gotting, K., Ross, E. & Sánchez Alvarado, A. SmedGD 2.0: the *Schmidtea mediterranea* genome database. *Genesis* **53**, 535–546 (2015).

nature research

Corresponding author(s): Marco Gallio

☐ Initial submission ☐ Revised version ☒ Final submission

Life Sciences Reporting Summary

Nature Research wishes to improve the reproducibility of the work that we publish. This form is intended for publication with all accepted life science papers and provides structure for consistency and transparency in reporting. Every life science submission will use this form; some list items might not apply to an individual manuscript, but all fields must be completed for clarity.

For further information on the points included in this form, see Reporting Life Sciences Research. For further information on Nature Research policies, including our data availability policy, see Authors & Referees and the Editorial Policy Checklist.

Experimental design

1. Sample size

Describe how sample size was determined.	The sample size was chosen based on literatures in the field.

2. Data exclusions

Describe any data exclusions.	No data were excluded from the analysis.

3. Replication

Describe whether the experimental findings were reliably reproduced.	Experimental findings were reliably reproduced

4. Randomization

Describe how samples/organisms/participants were allocated into experimental groups.	No randomization was used.

5. Blinding

Describe whether the investigators were blinded to group allocation during data collection and/or analysis.	Data collection and analysis were not performed blind to the conditions of the experiments.

Note: all studies involving animals and/or human research participants must disclose whether blinding and randomization were used.

6. Statistical parameters

For all figures and tables that use statistical methods, confirm that the following items are present in relevant figure legends (or in the Methods section if additional space is needed).

n/a	Confirmed	
☐	☒	The exact sample size (*n*) for each experimental group/condition, given as a discrete number and unit of measurement (animals, litters, cultures, etc.)
☐	☒	A description of how samples were collected, noting whether measurements were taken from distinct samples or whether the same sample was measured repeatedly
☐	☒	A statement indicating how many times each experiment was replicated
☐	☒	The statistical test(s) used and whether they are one- or two-sided (note: only common tests should be described solely by name; more complex techniques should be described in the Methods section)
☐	☒	A description of any assumptions or corrections, such as an adjustment for multiple comparisons
☐	☒	The test results (e.g. *P* values) given as exact values whenever possible and with confidence intervals noted
☐	☒	A clear description of statistics including central tendency (e.g. median, mean) and variation (e.g. standard deviation, interquartile range)
☐	☒	Clearly defined error bars

See the web collection on statistics for biologists for further resources and guidance.

Software

Policy information about availability of computer code

7. Software

Describe the software used to analyze the data in this study.	AxoGraph, Matlab, Image J.

For manuscripts utilizing custom algorithms or software that are central to the paper but not yet described in the published literature, software must be made available to editors and reviewers upon request. We strongly encourage code deposition in a community repository (e.g. GitHub). *Nature Methods* guidance for providing algorithms and software for publication provides further information on this topic.

Materials and reagents

Policy information about availability of materials

8. Materials availability

Indicate whether there are restrictions on availability of unique materials or if these materials are only available for distribution by a for-profit company.	All materials used in the work described in the manuscript are readily available from the authors or from standard commercial sources (Life Technologies, Ambion/ThermoFisher, Clontech, Promega, Fisher Scientific, Biotium, Sigma-Aldrich, Basler, MathWorks, Lonza, Qiagen, Axon Instruments, ALA Scientific Instruments, NPI Electronics, Physitemp Instruments, Genesee Scientific Inc, Molecular Probes, 20/20 Technology, National Instruments).

9. Antibodies

Describe the antibodies used and how they were validated for use in the system under study (i.e. assay and species).	The antibody that was used is a sheep anti-DIG-POD antibody (cat. # 11207733910, lot # 10520200, Sigma-Aldrich) The validation data is reported by the company that provides the antibody.

10. Eukaryotic cell lines

a. State the source of each eukaryotic cell line used.	Insect cells S2R+ were a gift from R. Carthew.
b. Describe the method of cell line authentication used.	The cells line has been authenticated by the donor.
c. Report whether the cell lines were tested for mycoplasma contamination.	The cell line was not tested for mycoplasma contamination because limited number of mycoplasma species able to replicate in insect cell cultures at 25 to 28° C (permissive temperature range for insect cells).
d. If any of the cell lines used are listed in the database of commonly misidentified cell lines maintained by ICLAC, provide a scientific rationale for their use.	No commonly misidentified cells lines were used.

Animals and human research participants

Policy information about studies involving animals; when reporting animal research, follow the ARRIVE guidelines

11. Description of research animals

Provide details on animals and/or animal-derived materials used in the study.	Schmidtea mediterranea (planarian worm, strain CIW4, asexual) and Drosophila melanogaster (fruit fly, various strains - see Materials and Methods, 3-5 days old, males and females)

Policy information about studies involving human research participants

12. Description of human research participants

Describe the covariate-relevant population characteristics of the human research participants.	N/A